

Right ventricular function in hypertrophic cardiomyopathy: A speckle tracking echocardiography study

Altuğ Cincin, Kürşat Tigen, Tansu Karaahmet¹, Cihan Dünder², Emre Gürel², Mustafa Bulut², Murat Sünbül, Yelda Başaran

Department of Cardiology, Faculty of Medicine, Marmara University; İstanbul-Turkey

¹Department of Cardiology, Faculty of Medicine, Acıbadem University; İstanbul-Turkey

²Department of Cardiology, Kartal Koşuyolu Heart Training and Research Hospital; İstanbul-Turkey

ABSTRACT

Objective: The aim of this study was to explore right ventricular (RV) mechanical function in patients with hypertrophic cardiomyopathy (HCM) by 2-D speckle tracking echocardiography (2-D-STE).

Methods: Forty-three patients with HCM (mean age 48, 17 females) and 40 healthy subjects were consecutively included in this cross-sectional study. The diagnosis of HCM was based on the presence of typical clinical, electrocardiographic (ECG), and echocardiographic features. Patients with LV systolic impairment, significant valvular disease, history of coronary artery disease, hypertension, malignancy, and chronic obstructive pulmonary disease were excluded. Right and left ventricular (LV) function was assessed by tissue Doppler imaging (TDI) and 2-D-STE. Hypertrophic cardiomyopathy patients were divided into two groups according to ACC/ESC guidelines (LVOT gradient below and above 30 mm Hg). Student t-test was used to compare differences between groups. Non-parametric tests (Mann-Whitney U) were used in cases of abnormal distribution.

Results: Hypertrophic cardiomyopathy patients had a significantly larger right atrium and RV diameters compared to controls. Mean pulmonary artery pressures (mPAB) were significantly higher in HCM patients (19.01±13.09 mm Hg vs. 8.40±4.50 mm Hg; p<0.001). Although RV Sm measurements were similar, RV strain measurements (-28.51±5.36% vs. -32.06±7.65%; p=0.016) were significantly lower in HCM patients. Left ventricular global longitudinal, radial, and circumferential strain values were also significantly different between the two groups (-20.50±3.58% vs. -24.12±3.40%; p<0.001, 38.18±12.67% vs. 44.80±10.15%; p=0.012, -21.94±4.28% vs. -23.91±3.95%; p=0.036 consecutively). Rotational movement of LV in each apical, mid-, and basal left ventricular segment was determined, and only mid-ventricular rotation of the HCM patients was more clockwise (-1.71±2.16 ° vs. 0.04±1.72 °; p<0.001). Although mPAP measurements were higher in HCM patients with significant LVOT obstruction (21.52±13.26 mm Hg vs. 12.31±10.53 mm Hg; p=0.049), none of the other TDI or 2-D-STE parameters was significantly different between groups.

Conclusion: Speckle tracking echocardiography-derived right ventricular systolic function is impaired in HCM patients when compared with healthy subjects. However, RV systolic function is not affected from LVOT obstruction and left ventricular rotation dynamics in HCM patients. (*Anatol J Cardiol* 2015; 15: 536-41)

Keywords: hypertrophic cardiomyopathy, right ventricular function, speckle tracking echocardiography

Introduction

Hypertrophic cardiomyopathy (HCM) is one of the primary diseases of the heart, characterized by impaired myocardial function despite increased left ventricle (LV) wall thickness (1). As the anatomical proximity emerges a clear functional relationship between two ventricles and genetic basis of the disease targets whole myocardium, right ventricular (RV) functional impairment accompany with the disease (2-4). However, evaluation of RV function with conventional echocardiographic techniques is unreliable because of the complex RV geometry, resulting in conflicting data.

Novel echocardiographic techniques offer reliable, reproducible, and quantitative information about right ventricle functions. Tricuspid annular systolic velocity (s) by TDI is well correlated with RV ejection fraction (EF), and isovolumic acceleration during isovolumic contraction (IVA) is proposed to be a useful index of RV contractile function and likely to be unaffected by preload and afterload changes in a physiological range (5, 6). Two-dimensional (2-D) speckle tracking echocardiography (2-D-STE) is an echocardiographic technique that uses standard 2-D images for detecting speckles (acoustic backscatters) in a previously determined region and is followed frame by frame (7). Multiple studies have demonstrated the utility of 2-D-STE in the



Address for Correspondence: Dr. Kürşat Tigen, Fevzi Çakmak Mahallesi, Fevzi Çakmak Mahallesi, Mimar Sinan Caddesi, No: 41 Üst Kaynarca, Pendik, İstanbul-Türkiye
Phone: +90 533 722 32 21 E-mail: mktigen@yahoo.com

Accepted Date: 09.05.2014 **Available Online Date:** 23.06.2014

© Copyright 2015 by Turkish Society of Cardiology - Available online at www.anatoljcardiol.com
DOI:10.5152/akd.2014.5538

evaluation of RV function without the limitation of a Doppler beam angle (8, 9). 2-D-STE was found to be a prognostic and clinical valuable tool in many heart diseases involving or affecting the RV (10-12).

The aim of our study was to evaluate RV functions in patients with obstructive and non-obstructive HCM and explore whether RV systolic function was affected by the disease itself or abnormal LV mechanics by using TDI and 2-D-STE parameters.

Methods

Fifty-six consecutive HCM patients underwent a clinical and echocardiographic examination in this cross-sectional study between 2010 and 2011 at Department of Cardiology, Faculty of Medicine, Marmara University. The diagnosis of HCM was based on the presence of typical clinical, electrocardiographic (ECG), and echocardiographic features, with global or segmental ventricular myocardial hypertrophy (diastolic wall thickness ≥ 15 mm), occurring in the absence of any other cardiac or systemic disease, such as Fabry's disease and cardiac amyloidosis (13).

Exclusion criteria were LV systolic impairment [ejection fraction (EF) $< 55\%$], significant valvular disease, history of coronary artery disease, hypertension, malignancy, chronic obstructive pulmonary disease, any arrhythmia that should affect echocardiographic measurements, and poor echocardiographic image quality. The study protocol was approved by the Ethic Committee.

Thirteen patients were excluded because of the criteria listed above, and 43 HCM patients were enrolled in the study; 40 healthy volunteers without any cardiac or systemic disease were matched for age and sex and included in the control group. Obstructive HCM was defined (in accordance with the latest American College of Cardiology guidelines) by the presence of a peak instantaneous gradient greater than 30 mm Hg from the ventricular cavity to the aorta under basal conditions (13).

Echocardiographic examination

All patients underwent a complete echocardiographic study with a commercially available echocardiography device (Vivid 7, GE Vingmed Ultrasound AS, Horten, Norway) by a single experienced cardiologist. Data acquisition was performed with a 3.5-MHz transducer at a depth of 14-18 cm in the parasternal and apical views (standard parasternal short-axis from basal, mid-ventricular, and apical levels; apical long-axis; two-chamber; and four-chamber views). Standard M-mode, 2-D, and color-coded tissue Doppler images (TDIs) were obtained during breath-hold, stored in cine-loop format from 3 consecutive beats, and transferred to a workstation for further offline analysis (EchoPAC 6.1; GE Vingmed Ultrasound AS). Gain settings, filters, and pulse repetitive frequency were adjusted to optimize color saturation, and a color Doppler frame scanning rate of 100-140 Hz was used for color TDI. Cardiac dimensions were measured according to the guidelines of the American Society of Echocardiography, and LV EF was calculated by biplane Simpson's method (14). Mean pulmonary artery pressure (mPAP)

was calculated with the acceleration time of the pulmonary artery velocity (Pact) by the Mahan formula [$mPAP$ (mm Hg) = $79 - (0.62 \times Pact$ (msn))] (15).

Pulsed TDI was performed to assess LV and RV longitudinal functions. In the apical four-chamber view, a 5-mm pulsed Doppler sample volume was placed on basal septum, basal lateral wall, and lateral tricuspid annulus. Settings were adjusted for a frame rate between 120 and 180 Hz, Nyquist velocity range of ± 20 cm/s, and horizontal record velocity of 90-100 m/s. Peak systolic velocity of the basal septum, basal lateral wall, and tricuspid lateral annulus (s); early and late diastolic velocities of LV septum and lateral wall; and isovolumetric contraction time (IVCT) and peak myocardial velocity during isovolumetric contraction (IVV) of the tricuspid lateral annulus were measured. LV systolic and early and late diastolic velocities were calculated by averaging the basal septal and lateral values. Isovolumetric acceleration (IVA) was calculated as the mean slope of the IVV wave (IVV/IVCT; m/s²) (6).

Multidirectional analysis of the LV [in the radial (GRS), circumferential (GCS), and longitudinal (GLS) directions] and RV strain was performed using 2-D speckle tracking imaging, as previously described (16-18). The assessment of GRS and GCS in the LV was performed by applying 2-D speckle tracking imaging to the parasternal short-axis views at a frame rate of 70-90 frame/s. The mid-ventricular short axis of the LV was divided into six segments, and the values of GRS and GCS were derived from the average of the six segmental peak systolic strain values. The assessment of longitudinal peak systolic strain was performed by applying 2-D speckle tracking imaging to the apical two- and four-chamber views of the LV. The LV was divided into six segments in each apical view. The values of GLS were derived from the average of the six segmental peak systolic longitudinal strain values.

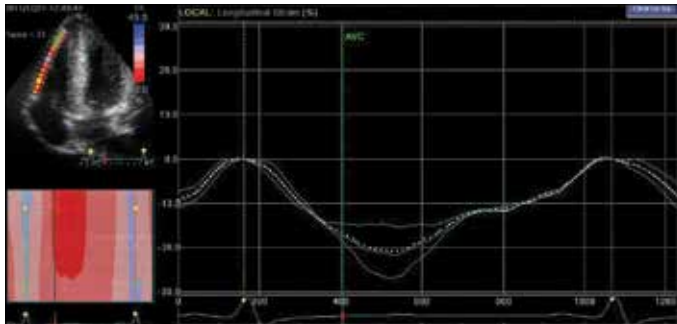
Two-dimensional speckle tracking analysis of the parasternal SAX views at the base and at the apex revealed LV 'rotation' and 'rotation rate' curves as the angular displacement and the velocity of displacement of the LV around its central axis. Negative values indicated clockwise rotation, while positive values indicated counterclockwise rotation. Left ventricular 'twist' and 'twist rate' were defined as the net difference of LV peak systolic 'rotation' and 'rotation rate' between basal (clockwise) and apical (counterclockwise) short axis planes. Values were expressed in 'degree (°)' and '°/s' respectively. 'Untwist' was expressed as a diastolic angular motion of the LV, opposite to twist. 'Untwisting rate' (°/s) was defined as the peak twist rate during early diastole. Midrotation was examined to detect the "null velocity" segment within the left ventricular cavity. The difference between left ventricular left ventricular mid and basal segment and basal segment rotation values was defined as midrotation, indicating the net twist between these segments.

For RV analysis, the free wall endocardial border of the ventricle, manually tracked on the end-systolic frame, and epicardial border were detected by the software. Strain curves and per-

Table 1. Basic clinical and echocardiographic parameters of the groups

	Patients with HCM (n=43)	Controls (n=40)	P
Age, years	47.79±14.94	46.57±11.18	0.678
Female sex	17	19	0.464
BSA, m ²	1.85±0.21	1.79±0.18	0.222
IVS, mm	22.51±5.81	10.06±1.46	<0.001
PW, mm	12.81±3.91	9.86±1.56	<0.001
LVEDD, mm	42.55±6.40	45.99±3.85	0.004
LVESD, mm	24.37±5.33	27.03±3.52	0.009
EF, %	73.69±9.10	71.15±5.78	0.135
E/A ratio	1.13±0.49	1.46±1.45	0.168
DT, ms	195±57	200±35	0.642
E/e ratio	19.8±8.6	9.6±2.7	<0.001
LVs, cm/s	5.55±1.46	7.76±1.68	<0.001
LVe, cm/s	5.02±2.10	9.38±2.18	<0.001
LVa, cm/s	5.82±1.87	8.01±2.12	<0.001
RA area, cm ²	12.97±2.24	11.91±2.65	0.055

BSA - body surface area; DT - deceleration time; EF - ejection fraction; IVS - interventricular septum thickness; LVEDD - left ventricular end-diastolic diameter; LVESD - left ventricular end-systolic diameter; LVa - left ventricular tissue Doppler late diastolic velocity; LVe - left ventricular tissue Doppler early diastolic velocity; LVs - left ventricular tissue Doppler systolic velocity; PW - posterior wall thickness; RA - right atrial

**Figure 1. Right ventricular strain analysis of an HCM patient by 2-D speckle tracking echocardiography**

centage of longitudinal differences at the basal segment of the RV free wall were obtained automatically (Fig. 1) (19, 20).

Statistical analysis

All statistical tests were performed with a commercially available statistical analysis program (SPSS 15.0 for Windows; SPSS, Inc., Chicago, IL, USA). All continuous variable results were checked for normal distribution by the Kolmogorov-Smirnov test and presented as mean±standard deviation (SD) or median (minimum-maximum values), while categorical variables were expressed as ratios. Student t-test was used to compare difference between groups. Non-parametric tests (Mann-Whitney U) were used in cases of abnormal distribution. Correlation analysis was performed by Spearman's correlation test. A p value of <0.05 was determined as statistically significant. Intraobserver (the mean difference between two independent measurements)

Table 2. Doppler and 2D-STE indices of the groups

	Patients with HCM (n=43)	Controls (n=40)	P
Pacc, ms	96.75±21.12	113.86±7.27	<0.001
mPAB, mm Hg	19.01±13.09	8.40±4.50	<0.001
RVs, cm/s	11.62±2.66	12.40±2.22	0.153
RV IVV, cm/s	7.97±3.32	8.97±2.83	0.154
RV IVA, cm/s ²	1.89±0.74	2.48±0.67	0.001
RV BLS, %	-28.51±5.36	-32.06±7.65	0.016
LV GLS, %	-20.50±3.58	-24.12±3.40	<0.001
LV GRS, %	38.18±12.67	44.80±10.15	0.012
LV GCS, %	-21.94±4.28	-23.91±3.95	0.036
LV rot-apical, °	15.93±7.16	15.84±5.38	0.952
LV rot-mid, °	-1.71±2.16	0.04±1.72	<0.001
LV rot-basal, °	-6.38±2.90	-6.75±3.33	0.594
LV twist, °	22.37±6.77	22.29±6.22	0.955
LV untwist, °/s	-122.57±51.72	-135.64±38.93	0.209

BLS - free wall basal segment longitudinal strain; GCS - global circumferential strain; GLS - global longitudinal strain; GRS - global radial strain; IVA - isovolumic acceleration during isovolumic contraction; IVV - peak isovolumetric contraction velocity; LV - left ventricle; mPAP - mean pulmonary artery pressure; Pacc - pulmonary acceleration time; rot - rotation; RV - right ventricle; RVs - peak systolic velocity of tricuspid lateral annulus

and interobserver (the mean difference between two independent observers) variabilities were analyzed in 10 randomly selected studies and expressed as the mean percent error (difference divided by number of observations).

Results

Forty-three patients with HCM (mean age 48, 17 females) and 40 healthy subjects (mean age 47, 19 females) were included in the study. Demographic and conventional echocardiographic parameters are presented in Table 1. The groups were not significantly different in terms of cardiovascular risk factors. Interventricular septum (IVS) and posterior wall measurements in the HCM group were 22.51±5.81 mm and 12.81±3.91 mm, respectively. Left ventricular ejection fraction values were not different between HCM patients and the control group.

Doppler, TDI, and 2-D-STE results of the groups are shown in Table 2. Estimated mPAP was higher in HCM patients (19.01±13.09 mm Hg vs. 8.40±4.50 mm Hg; p<0.001). Although RVs (11.62±2.66 cm/s vs. 12.40±2.22 cm/s; p=0.153) and IVV (7.97±3.32 cm/s vs. 8.97±2.83 cm/s; p=0.154) measurements were similar, IVA (1.89±0.74 cm/s² vs. 2.48±0.67 cm/s²; p=0.001) and strain measurements of the basal RV free wall (-28.51±5.36% vs. -32.06±7.65%; p=0.016) were significantly lower in HCM patients. The estimated inter- and intra-observer variability for RVs and strain of basal RV free wall measurements were 2.3% and 3.1% versus 2.8% and 3.4%, respectively. Left ventricular GLS, GRS, and GCS values between groups were also significantly different (-20.50±3.58% vs. -24.12±3.40%; p<0.001,

38.18±12.67% vs. 44.80±10.15%; p=0.012, -21.94±4.28% vs. -23.91±3.95%; p=0.036, consecutively). Rotational movement of the LV in each apical, mid-, and basal segment was determined, and only mid-ventricular rotation of the HCM group patients was more clockwise in the HCM group (-1.71±2.16° vs. 0.04±1.72°; p<0.001).

Hypertrophic cardiomyopathy patients were divided into two groups according to their LV outflow tract gradient. Thirty-two of

Table 3. Doppler and 2D-STE indices of HCM patients, according to LV outflow gradients

	Patients with obstruction (n=32)	Patients without obstruction (n=11)	P
Pacc, ms	92.70±21.39	107.55±16.99	0.049
mPAB, mm Hg	21.52±13.26	12.31±10.53	0.049
E/A ratio	1.09±0.45	1.23±0.59	0.432
E/e ratio	20.4±9.4	18.3±7.2	0.496
LVs, cm/s	5.78±1.52	4.88±1.08	0.078
LVe, cm/s	5.17±2.29	4.58±1.41	0.427
LVa, cm/s	6.07±1.93	5.09±1.56	0.137
RVs, cm/s	11.71±2.55	11.36±3.10	0.714
RV IVV, cm/s	8.01±3.13	7.86±3.96	0.899
RV IVA, cm/s ²	1.88±0.77	1.92±0.72	0.887
RV BLS, %	-27.95±5.36	-30.15±5.26	0.246
LV GLS, %	-20.31±3.37	-21.07±4.28	0.550
LV GRS, %	38.31±13.62	37.86±10.31	0.923
LV GCS, %	-22.35±4.33	-20.87±4.12	0.336
LV rot-apical, °	16.68±6.92	16.60±8.07	0.720
LV rot-mid, °	-1.92±2.16	-1.16±2.17	0.331
LV rot-basal, °	-6.23±3.09	-6.76±2.44	0.714
LV twist, °	22.52±6.48	21.99±6.53	0.728
LV untwist, °/s	-132.78±41.00	-122.53±53.78	0.343

BLS - free wall basal segment longitudinal strain; GCS - global circumferential strain; GLS - global longitudinal strain; GRS - global radial strain; IVA - isovolumic acceleration during isovolumic contraction; IVV - peak isovolumetric contraction velocity; LV - left ventricle; LVa - left ventricular tissue Doppler late diastolic velocity; LVe - left ventricular tissue Doppler early diastolic velocity; LVs - left ventricular tissue Doppler systolic velocity; mPAP - mean pulmonary artery pressure; Pacc - pulmonary acceleration time; rot - rotation; RV - right ventricle; RVs - peak systolic velocity of tricuspid lateral annulus

the 43 HCM patients whose peak LVOT gradients were higher than 30 mm Hg, were assigned as obstructive. Echocardiographic findings of obstructive and non-obstructive patients are shown in Table 3. Pulmonary acceleration time (92.70±21.39 ms vs. 107.55±16.99 ms; p=0.049) and mPAP measurements (21.52±13.26 mm Hg vs. 12.31±10.53 mm Hg; p=0.049) were higher in HCM patients with LVOT obstruction. Tissue Doppler and STE measurements of RV did not reveal significant difference between obstructive and non-obstructive HCM patients according to an LVOT gradient threshold of 30 mm Hg. RVs (11.71±2.55 cm/s vs. 11.36±3.10 cm/s; p=0.714), IVV (8.01±3.13 cm/s vs. 7.86±3.96 cm/s; p=0.899), and IVA (1.88±0.77 cm/s² vs. 1.92±0.72 cm/s²; p=0.887) were similar. Strain measurements of the basal RV free wall (-27.95±5.36% vs. -30.15±5.26%; p=0.246) were similar between the two groups.

Another comparison was performed by separating HCM patients according to their direction of mid-ventricular rotation. Counter-clockwise rotation was seen in 8 of the 43 patients, and clockwise rotation was seen in the remaining patients. There was no difference between the two groups in terms of RV functional parameters. Right-sided echocardiographic parameters were evaluated according to mid-ventricular rotation quartiles. Table 4 shows the comparisons between quartiles. Among the evaluated parameters, no significant difference was detected between mid-ventricular rotation quartiles or the 1st and 4th quartiles.

Discussion

In our study, significant impairment in RV function was demonstrated in HCM patients by using 2-D-STE when compared with age- and sex-matched healthy volunteers. Although tissue Doppler-derived systolic velocity of the tricuspid lateral annulus did not differ between groups, 2-D-STE-based strain of the RV free wall basal segment in the HCM group was lower in HCM patients. Although the calculated mPAP values were higher, patients who had LVOT outflow tract obstruction were found to have similar RV systolic function parameters compared to patients without LVOT obstruction. Mid-ventricular rotation of the LV was significantly clockwise in HCM patients compared to controls but similar between obstructed and non-obstructed HCM patients. HCM patients were analyzed according to their

Table 4. Doppler and 2D-STE indices of HCM patients, according to interquartile ranges of mid-ventricular rotation values

	1. Quartile n=10	2. Quartile n=10	3. Quartile n=10	4. Quartile n=10	P (overall)	P (1 st and 4 th quartiles)
Pacc, ms	107.50±18.3	90±30.62	98.33±16.00	91.62±19.38	0.317	0.130
mPAB, mm Hg	12.35±11.39	23.20±18.98	18.03±9.92	22.19±12.01	0.317	0.130
RVs, cm/s	11.94±2.68	10.98±2.33	12.29±2.57	11.26±3.18	0.715	0.739
RV IVV, cm/s	7.75±3.00	7.04±3.37	7.87±4.04	8.72±3.05	0.714	0.573
RV IVA, cm/s ²	2.18±0.72	1.62±0.68	1.60±0.87	2.23±0.56	0.134	0.696
RV BLS, %	-28.26±0.30	-27.35±5.36	-30.36±4.82	-27.55±4.09	0.359	0.529

BLS - free wall basal segment longitudinal strain; IVA - isovolumic acceleration during isovolumic contraction; IVV - peak isovolumetric contraction velocity; mPAP - mean pulmonary artery pressure; Pacc - pulmonary acceleration time; RV - right ventricle; RVs - peak systolic velocity of tricuspid lateral annulus

quartiles of mid-ventricular rotation, and no significant difference in terms of RV parameters between mid-rotation quartiles was found.

RV function is affected in HCM as a consequence of the direct disease itself, ventricular interdependence, or dynamic afterload changes (2, 21-23). Although the morphological and physiological changes of the LV in HCM are well described, the right heart is obscured by its complex geometry and physiology (24, 25). The clear prognostic importance of RV function in various diseases has encouraged investigations about new echocardiographic methods for accurate diagnosis of RV failure (26-28). In a recently published article, D'andrea et al. (29) showed that 2-D-STE-derived RV myocardial systolic deformation is influenced in HCM patients. There was a negative association between inter-ventricular septal thickness and RV global longitudinal strain in HCM patients. Our results also suggested impairment in STE-derived RV systolic function when compared with normal subjects.

LV obstruction and right heart functions

In patients with HCM and LVOT obstruction, increased LV loading conditions and diastolic dysfunction have an important effect in RV workload (30). A study in patients treated with alcohol septal ablation showed that eliminating LVOT obstruction was related with decreased PAP and increased RV ejection fraction values (31). In our study, patients with LVOT obstruction had higher pulmonary artery pressures. However, TDI- or 2-D-STE-based RV systolic function parameters were similar between obstructed and non-obstructed patients. This might be due to mild elevation of pulmonary artery pressures in our HCM patients. LVOT obstruction was not related with impairment in LV strain and rotation parameters in our patient group. This might preserve the left atrial and pulmonary artery pressures and maintain RV systolic function within normal limits. Our findings need to be clarified by further large-scale follow-up studies.

Mid-ventricular rotation and right ventricle functions

In a study made by Carasso et al. (32), HCM patients with preserved systolic function were associated with impaired STE-derived LV longitudinal strain, unchanged LV torsion, and increased circumferential strain. However, mid-ventricular mechanical analysis of HCM patients revealed a clockwise rotation pattern, despite "mid-ventricular null velocity." To the best of our knowledge, this is the first study evaluating the effect of this diversity on RV functions. In our study, similar to the Carasso et al. (32) results, mid-cavity rotational motion was significantly different between control and HCM patients. However, RV systolic function was not affected from the mid-ventricular rotation pattern. A detailed analysis was performed by dividing the HCM group into mid-rotation quartiles, which showed similar RV strain values. Preservation of LV systolic parameters and a mild elevation in pulmonary artery pressures might be an explanation for these findings. The relation between mid-rotation and RV systolic parameters in HCM patients with advanced disease indicates further research.

Study limitations

The main limitation of our study was the small sample size. Although the difference in RV BLS between HCM patients and controls was significant, whole measurements were within the normal range, as previously established (33). The importance of these sub-clinical findings should be determined with a prospective study, including prognosis.

Morphologic changes in the RV itself are another important factor affecting functions in HCM patients, but these changes were not considered in the present study. Cardiac MRI might be used to validate both RV systolic functions and morphologic changes, like fibrosis.

Conclusion

Speckle tracking echocardiography-derived right ventricular systolic function is impaired in HCM patients when compared with healthy subjects. However, RV systolic function is not affected from LVOT obstruction and left ventricular rotation dynamics in HCM patients.

Conflict of interest: None declared.

Peer-review: Externally peer-reviewed.

Authorship contributions: Concept - Y.B., K.T.; Design - K.T.; Supervision - A.C., T.K.; Data collection and/or processing - C.D., A.C., E.G.; Analysis and/or Interpretation - M.B., A.C., M.S.; Literature search - T.K.; Writing - A.C., K.T.; Critical review - Y.B.

References

1. Elliott P, Andersson B, Arbustini E, Bilinska Z, Cecchi F, Charron P, et al. Classification of the cardiomyopathies: a position statement from the European Society of Cardiology Working Group on Myocardial and Pericardial Diseases. *Eur Heart J* 2008; 29: 270-6. [\[CrossRef\]](#)
2. Prinz C, van Buuren F, Faber L, Bitter T, Bogunovic N, Burchert W, et al. Myocardial fibrosis is associated with biventricular dysfunction in patients with hypertrophic cardiomyopathy. *Echocardiography* 2012; 29: 438-44. [\[CrossRef\]](#)
3. Maron MS, Hauser TH, Dubrow E, Horst TA, Kissinger KV, Udelson JE, et al. Right ventricular involvement in hypertrophic cardiomyopathy. *Am J Cardiol* 2007; 100: 1293-8. [\[CrossRef\]](#)
4. Zemanek D, Tomasov P, Prichystalova P, Linhartova K, Veselka J. Evaluation of the right ventricular function in hypertrophic obstructive cardiomyopathy: a strain and tissue Doppler study. *Physiol Res* 2010; 59: 697-702.
5. Sato T, Tsujino I, Ohira H, Oyama-Manabe N, Yamada A, Ito YM, et al. Validation study on the accuracy of echocardiographic measurements of right ventricular systolic function in pulmonary hypertension. *J Am Soc Echocardiogr* 2012; 25: 280-6. [\[CrossRef\]](#)
6. Vogel M, Schmidt MR, Kristiansen SB, Cheung M, White PA, Sorensen K, et al. Validation of myocardial acceleration during isovolumic contraction as a novel noninvasive index of right ventricular contractility: comparison with ventricular pressure-volume relations in an animal model. *Circulation* 2002; 105: 1693-9. [\[CrossRef\]](#)

7. Mor-Avi V, Lang RM, Badano LP, Belohlavek M, Cardim NM, Derumeaux G, et al. Current and evolving echocardiographic techniques for the quantitative evaluation of cardiac mechanics: ASE/EAE consensus statement on methodology and indications endorsed by the Japanese Society of Echocardiography. *J Am Soc Echocardiogr* 2011; 24: 277-313. [\[CrossRef\]](#)
8. Langeland S, D'Hooge J, Wouters PF, Leather HA, Claus P, Bijmens B, et al. Experimental validation of a new ultrasound method for the simultaneous assessment of radial and longitudinal myocardial deformation independent of insonation angle. *Circulation* 2005; 112: 2157-62. [\[CrossRef\]](#)
9. Ahmad H, Mor-Avi V, Lang RM, Nesser HJ, Weinert L, Tsang W, et al. Assessment of right ventricular function using echocardiographic speckle tracking of the tricuspid annular motion: comparison with cardiac magnetic resonance. *Echocardiography* 2012; 29: 19-24. [\[CrossRef\]](#)
10. Sünbül M, Kepez A, Kıvrak T, Eroğlu E, Özben B, Yıldızeli B, et al. Right ventricular longitudinal deformation parameters and exercise capacity: Prognosis of patients with chronic thromboembolic pulmonary hypertension. *Herz* 2013 Jun 7. Epub ahead of print.
11. Kusunose K, Popovic ZB, Motoki H, Marwick TH. Prognostic significance of exercise-induced right ventricular dysfunction in asymptomatic degenerative mitral regurgitation. *Circ Cardiovasc Imaging* 2013; 6: 167-76. [\[CrossRef\]](#)
12. Iacoviello M, Puzzovivo A, Guida P, Forleo C, Monitillo F, Catanzaro R, et al. Independent role of left ventricular global longitudinal strain in predicting prognosis of chronic heart failure patients. *Echocardiography* 2013; 30: 803-11. [\[CrossRef\]](#)
13. Maron BJ, McKenna WJ, Danielson GK, Kappenberger LJ, Kuhn HJ, Seidman CE, et al. American College of Cardiology/European Society of Cardiology clinical expert consensus document on hypertrophic cardiomyopathy. A report of the American College of Cardiology Foundation Task Force on Clinical Expert Consensus Documents and the European Society of Cardiology Committee for Practice Guidelines. *J Am Coll Cardiol* 2003; 42: 1687-713. [\[CrossRef\]](#)
14. Cheitlin MD, Armstrong WF, Aurigemma GP, Beller GA, Bierman FZ, Davis JL, et al. ACC/AHA/ASE 2003 Guideline Update for the Clinical Application of Echocardiography: summary article. A report of the American College of Cardiology/American Heart Association Task Force on Practice Guidelines (ACC/AHA/ASE Committee to Update the 1997 Guidelines for the Clinical Application of Echocardiography). *J Am Soc Echocardiogr* 2003; 16: 1091-110. [\[CrossRef\]](#)
15. Dabestani A, Mahan G, Gardin JM, Takenaka K, Burn C, Allfie A, et al. Evaluation of pulmonary artery pressure and resistance by pulsed Doppler echocardiography. *Am J Cardiol* 1987; 59: 662-8. [\[CrossRef\]](#)
16. Delgado V, Ypenburg C, van Bommel RJ, Tops LF, Mollema SA, Marsan NA, et al. Assessment of left ventricular dyssynchrony by speckle tracking strain imaging comparison between longitudinal, circumferential, and radial strain in cardiac resynchronization therapy. *J Am Coll Cardiol* 2008; 51: 1944-52. [\[CrossRef\]](#)
17. Donal E, Tournoux F, Leclercq C, De Place C, Solnon A, Derumeaux G, et al. Assessment of longitudinal and radial ventricular dyssynchrony in ischemic and nonischemic chronic systolic heart failure: a two-dimensional echocardiographic speckle-tracking strain study. *J Am Soc Echocardiogr* 2008; 21: 58-65. [\[CrossRef\]](#)
18. Cameli M, Righini FM, Lisi M, Mondillo S. Right ventricular strain as a novel approach to analyze right ventricular performance in patients with heart failure. *Heart Fail Rev* 2013 Nov 28. Epub ahead of print.
19. Leung DY, Ng AC. Emerging clinical role of strain imaging in echocardiography. *Heart Lung Circ* 2010; 19: 161-74. [\[CrossRef\]](#)
20. Blessberger H, Binder T. Two-dimensional speckle tracking echocardiography: clinical applications. *Heart* 2010; 96: 2032-40. [\[CrossRef\]](#)
21. Mandysova E, Niederle P. Influence of load changes on tricuspid inflow. *Physiol Res* 2007; 56: 299-305.
22. McKenna WJ, Kleinebenne A, Nihoyannopoulos P, Foale R. Echocardiographic measurement of right ventricular wall thickness in hypertrophic cardiomyopathy: relation to clinical and prognostic features. *J Am Coll Cardiol* 1988; 11: 351-8. [\[CrossRef\]](#)
23. Santamore WP, Dell'Italia LJ. Ventricular interdependence: significant left ventricular contributions to right ventricular systolic function. *Prog Cardiovasc Dis* 1998; 40: 289-308. [\[CrossRef\]](#)
24. Lang RM, Bierig M, Devereux RB, Flachskampf FA, Foster E, Pellikka PA, et al. Recommendations for chamber quantification: a report from the American Society of Echocardiography's Guidelines and Standards Committee and the Chamber Quantification Writing Group, developed in conjunction with the European Association of Echocardiography, a branch of the European Society of Cardiology. *J Am Soc Echocardiogr* 2005; 18: 1440-63. [\[CrossRef\]](#)
25. Maron BJ. Hypertrophic cardiomyopathy: a systematic review. *JAMA* 2002; 287: 1308-20. [\[CrossRef\]](#)
26. Severino S, Caso P, Cicala S, Galderisi M, de Simone L, D'Andrea A, et al. Involvement of right ventricle in left ventricular hypertrophic cardiomyopathy: analysis by pulsed Doppler tissue imaging. *Eur J Echocardiogr* 2000; 1: 281-8. [\[CrossRef\]](#)
27. Mehta SR, Eikelboom JW, Natarajan MK, Diaz R, Yi C, Gibbons RJ, et al. Impact of right ventricular involvement on mortality and morbidity in patients with inferior myocardial infarction. *J Am Coll Cardiol* 2001; 37: 37-43. [\[CrossRef\]](#)
28. Galderisi M, Severino S, Cicala S, Caso P. The usefulness of pulsed tissue Doppler for the clinical assessment of right ventricular function. *Ital Heart J* 2002; 3: 241-7.
29. D'Andrea A, Caso P, Bossone E, Scarafilo R, Riegler L, Di Salvo G, et al. Right ventricular myocardial involvement in either physiological or pathological left ventricular hypertrophy: an ultrasound speckle-tracking two-dimensional strain analysis. *Eur J Echocardiogr* 2010; 11: 492-500. [\[CrossRef\]](#)
30. Timmer SA, Knaepen P, Germans T, Lubberink M, Dijkmans PA, Vonk-Noordegraaf A, et al. Right ventricular energetics in patients with hypertrophic cardiomyopathy and the effect of alcohol septal ablation. *J Card Fail* 2011; 17: 827-31. [\[CrossRef\]](#)
31. Wang J, Buegler JM, Veerasamy K, Ashton YP, Nagueh SF. Delayed untwisting: the mechanistic link between dynamic obstruction and exercise tolerance in patients with hypertrophic obstructive cardiomyopathy. *J Am Coll Cardiol* 2009; 54: 1326-34. [\[CrossRef\]](#)
32. Carasso S, Yang H, Woo A, Vannan MA, Jamorski M, Wigle ED, et al. Systolic myocardial mechanics in hypertrophic cardiomyopathy: novel concepts and implications for clinical status. *J Am Soc Echocardiogr* 2008; 21: 675-83. [\[CrossRef\]](#)
33. Meris A, Faletra F, Conca C, Klersy C, Regoli F, Klimusina J, et al. Timing and magnitude of regional right ventricular function: a speckle tracking-derived strain study of normal subjects and patients with right ventricular dysfunction. *J Am Soc Echocardiogr* 2010; 23: 823-31. [\[CrossRef\]](#)